Design and Experimental Investigation of Temperature Control for a 10 kW SOFC System Based on an Artificial Neuronal Network

N. Kruse[a], W. Tiedemann[a], I. Hoven[a], R. Deja[a], Ro. Peters[a], F. Kunz[a], and R.-A. Eichel[a,b]

[a] Forschungszentrum Jülich GmbH, Institute of Energy and Climate Research (IEK-9), 52428 Jülich, Germany
[b] RWTH Aachen University, Institute of Physical Chemistry, Templergraben 55, 52074 Aachen, Germany

In this work the authors designed and experimentally evaluated different controller topologies for fuel cell operation (SOFC) of a reversible solid oxide cell (rSOC) system. Aim of the controller is to operate the SOFC system autonomously at a constant maximum temperature for maximum efficiency. The controller design incorporates an artificial neuronal network (ANN) for real time state predictions. The training data for the ANN was generated by a Digital Twin of this system. The generated training data consists of about 16,000 different steady state operating conditions.

Introduction

For a future carbon-neutral energy economy, fuel cells play an important role due their high efficiency. Especially the Solid Oxide Fuel Cell (SOFC) with demonstrated efficiencies beyond 60 % [1] can contribute to reasonable roundtrip efficiencies for hydrogen and e-fuels [2].

To match the fluctuating electricity demand and generation in a future electricity grid, dominated by renewable energy sources like wind and photovoltaic, dynamic operation of fuel cells is required. Previous research has shown that the degradation und therefore the lifespan of Solid Oxide Cell (SOC) stacks shows a significant dependency on the operating conditions and dynamic load changes [3]. However, some research suggests that the degradation is not caused by the load changes itself but spatial temperature gradients during load changes [4–6].

Therefore, controlling the temperature gradients in the stack during load changes can have a significant impact on the lifespan of SOC stacks. This is typically more dramatically for stacks with larger footprints. For systems with heat exchangers to recover heat from the off gases to heat up the hydrogen and air stream the efficiency in fuel cell operation improves with increasing stack temperature due to lowering the cell resistances and therefore the losses. The upper temperature limit is determined by the stack materials, in particular the glass-ceramic seal. Exceeding the given limits locally in the stack can result in a total failure or accelerated degradation. Therefore, a tight temperature control allows for running the stack at maximum efficiency without the risk of stack damage by exceeding temperature limits.

The challenge is to keep the temperature during load changes at the location with the maximum temperature almost constant and below the limit. For most SOC system designs the only degree of freedom for controlling the temperature for a given cell current or output power at maximum efficiency is the air flow rate. If a fuel recirculation is used, the recirculation flow may be an additional option, but is usually less favorable for temperature control du to other constrains. Therefore, this work focuses on the air flow rate.

Experimental

This work is divided in two parts. In the first part we present a simple approach to robustly control the stack temperature at steady state operation. In the second part this method is extended with an artificial neuronal network (ANN) to provide a feedback-controlled stack temperature over large range of operating conditions.

The controllers were tested and evaluated at an 10/40 kW reversible solid oxide cell (rSOC) system [7] operated in fuel cell mode. Figure 1 shows a simplified flow scheme for the SOFC operation mode of the system. The Integrated Module (IM) contains a stack with a total of up to 80 layers, as well as heat exchangers for the preheating of fuel and air. The active cell area per layer is about 320 cm². The stack is operated in co-flow, whereas the heat exchangers are operated in counter-flow configuration.

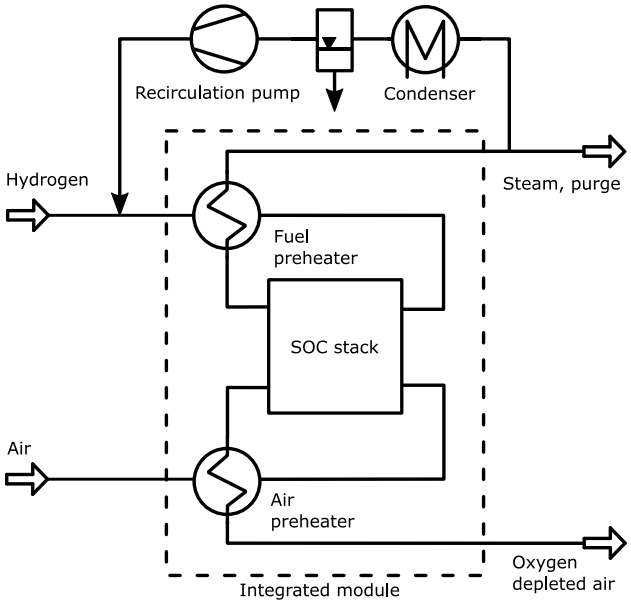

Figure 1. Configuration of the rSOC system for SOFC operation

The previous developed LabVIEW program for operating the system manually has been extended with an interface based on Modbus/TCP to couple the system with the experimental controllers written in Python/TensorFlow (Figure 2). By using a TCP/IP based interface a maximum of flexibility can be achieved. This allows for example to run the controller remotely on hardware equipped with GPU acceleration.

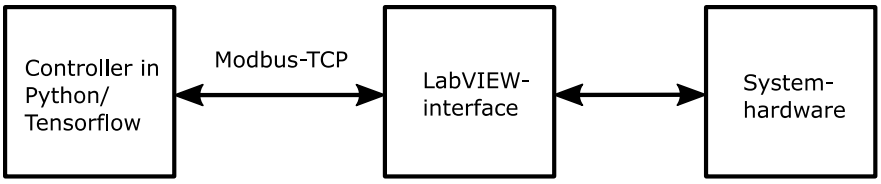

Figure 2. Controller interface for the rSOC system

Steady State Control

For steady state operation the air flow rate must be controlled in such a way the total enthalpy of the IM stays constant. Therefore, the sum of all energy and enthalpy flows must be zero (Equation 1).

$$0 = \sum (\dot{n}_{i,in} \cdot h_{i,in} - \dot{n}_{i,out} \cdot h_{i,out}) + (\dot{n}_{H2,in} - \dot{n}_{H2,out}) \cdot LHV + P_{el} + \dot{Q}_{loss} \qquad [1]$$

$\dot{n}_{i,in}$	Molar flow of species *i* at the inlet of the IM
$\dot{n}_{i,out}$	Molar flow of species *i* at the outlet of the IM
$h_{i,in}$	Specific enthalpy at inlet conditions of species *i*
$h_{i,out}$	Specific enthalpy at outlet conditions of species *i*
LHV	Lower heating value of hydrogen
P_{el}	Generated electrical power at the stack
$\dot{Q}_{loss}$	Heat loss through insolation of the IM

A conventional PID controller can't be used to control the maximum stack temperature, due to positive feedback effects in the relevant frequency band. Lowering the maximum stack temperature long-term requires an increase in air flow rate. However, an increasing air flow rate has the effect that the stack cools down at the air inlet, which lowers the local current density due to increasing cell resistance. Keeping the total stack current or power constant, implies therefore an increasing current density and therefore heat production at the center and outlet side of the stack. This is typically the hottest stack region. Increasing the air flow rate increases temporarily the maximum stack temperature but lowers it long therm.

This effect applies for feedback controlling the maximum stack temperature. However, to keep the total enthalpy of the stack constant it is sufficient to control a measurable variable witch is proportional to the stack enthalpy. In this work we achieved this by calculating a weighted average (T_{av}) based on 13 temperature measurements (T_i) distributed over the stacks and heat exchangers of the IM. The individual weights are assigned by dividing the IM in 13 sub sections belonging to the measured temperature. The weight for each temperature is then based on its fraction of the total heat capacity (C_i/C_{total}) of the IM (Equation 2).

$$T_{av} = \frac{1}{C_{total}} \sum_{i=0}^{13} T_i \cdot C_i \qquad [2]$$

This weighted average temperature is proportional to the integral over time of the right-side term of equation 1 (designated as $\dot{Q}_{excess}$ in the following). Therefore, the dependency between the weighted average temperature and air flow rate can be described as a first order differential equation:

$$\frac{\mathrm{d}T_{av}}{\mathrm{d}t} = \frac{\dot{Q}_{excess}}{C_{total}} \qquad [3]$$

Such a system can be well controlled by a conventional PID controller.

Artificial Neuronal Network Controller

For varying operation conditions, the described method is no longer sufficient for controlling the maximum stack temperature. The temperature span in the stack increases with rising current density. Therefore, keeping the local maximum temperature in the stack constant requires lowering the temperature in other regions of the stack. This necessitates additional cooling of the stack during an increase of current density.

For maintaining the robustness of the previous descripted approach based on controlling the average temperature of the IM and adapting the temperature profile for varying operation conditions a cascaded approach as shown in Figure 3 was chosen.

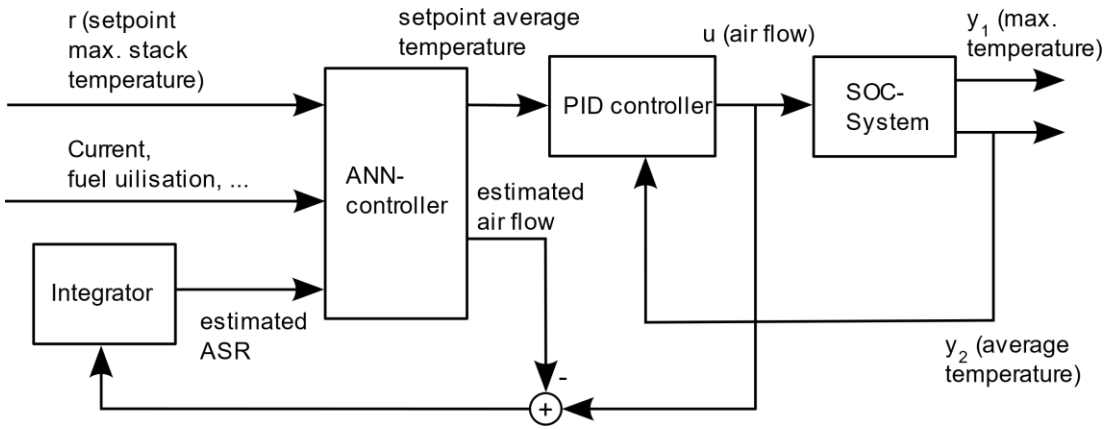

Figure 3. ANN based cascaded temperature controller

While the average temperature (y_2) is still controlled by the PID controller as described above, the setpoint for the average temperature is determined by an ANN. The ANN is supposed to output an average temperature. The input parameters for the ANN are the setpoint for the maximum stack temperature (r), the momentary current density, fuel utilization of the system, recirculation ratio and an estimated prefactor (A) for the temperature dependent area specific resistance (ASR) as shown in Equation 4.

$$ASR = A \cdot e^{\frac{E_A}{RT}} \qquad [4]$$

A	Prefactor for describing degradation state of the stack
E_A	Parameter for temperature dependency expressed as activation energy
RT	Product of universal gas constant and local stack temperature

The ASR prefactor A is estimated and tracked by integration of the difference between actual air flow rate and predicted air flow rate.

To train the ANN, artificial training data was generated by a Digital Twin of the system. This model [8,9] is implemented in Matlab Simulink and was validated against experimental data. The generated training data consists of 16,000 different steady state operating conditions of the system. The ASR value was varied as well.

The ANN uses dense layers with Exponential Linear Unit (elu) activations and skip connections as shown in Figure 4. It is implemented in TensorFlow and was trained on a NVIDIA A30 GPU with a batch size of 262144. Training and validation loss improved for about 400 epochs and stayed then constant for more than 1400 epochs. No indications for overfitting where observed. The input data consists of normalized current density, fuel utilization, recirculation ratio, maximum stack temperature and a prefactor for the ASR. The model outputs a normalized steady state air flow rate and average temperature.

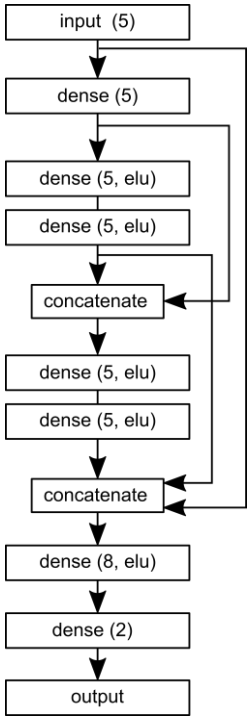

Figure 4. Layout of the ANN based on fully connected layers with elu activation

Results and Discussion

Both controllers were evaluated and tested for fuel cell operation with a current density profile between 0.3 and 0.5 A/cm² and a current change rate of 0.19 A/cm²/h. The experiments were carried out with the described rSOC system. The following results are based on a reduced stack size from originally 80 to 60 cell layers. This reduction was necessary after a partial stack failure. The PID controller for constant average temperature control showed as expected an excellent control behavior concerning the average temperature of the Integrated Module as shown in Figure 5.

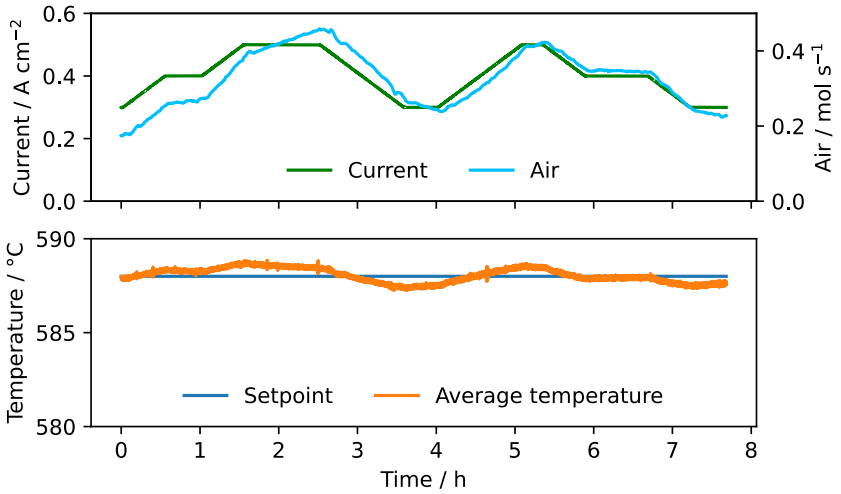

Figure 5. Experimental results of the PID controller controlling the average temperature of the Integrated Module

However, while the average temperature is tightly controlled, the maximum stack temperature still changes significantly with the current density as shown in Figure 6. It is to note, that the weighted average temperature (shown in Figure 5) is not only calculated from the listed stack temperatures in Figure 6, but although from two temperatures measured in the air preheater and two in the fuel preheater of the IM. The shown temperatures T1, T4 and T7 are measured at the inlet side of the stack, T2, T5 and T8 at the center and the T3, T6 and T9 at the outlet side.

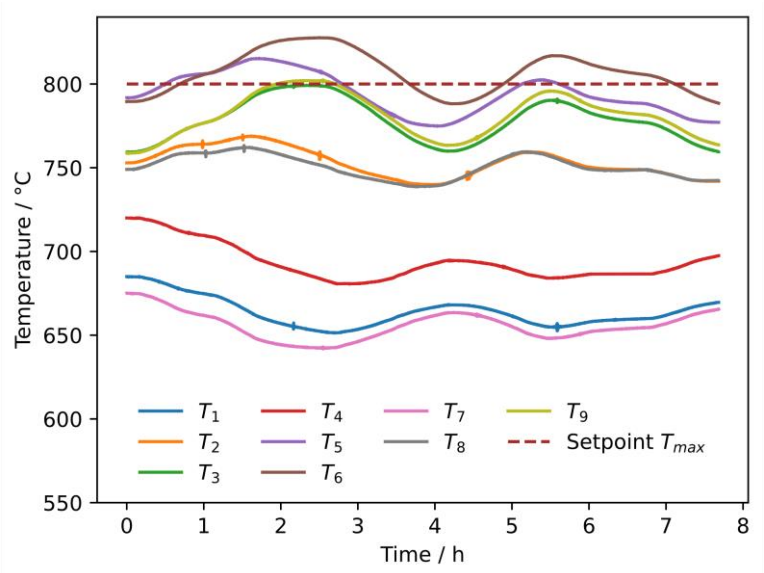

Figure 6. Stack temperature change with variation of current density at constant average temperature

The results from operation of the cascaded controller, where the average temperature is determined by the ANN are shown in Figures 7 and 8. Due to the requirement of keeping the maximum temperature constant, the average temperature must be decreased during current increase and increase vice versa. This is reflected by the higher modulation range for the resulting air flow rate.

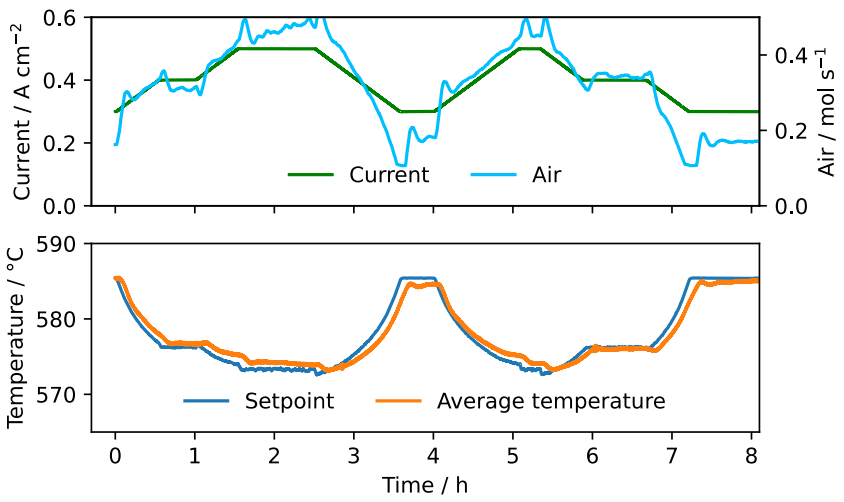

Figure 7. Experimental results of the cascaded ANN controller

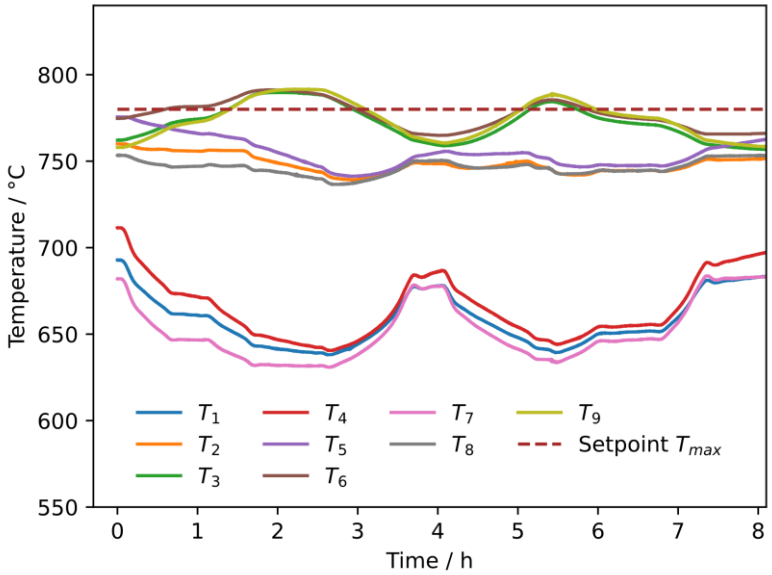

Figure 8. Stack temperature change with variation of current density at constant maximum temperature

As shown in Figure 8 the fluctuation of the maximum temperature can be significantly reduced with the proposed ANN controller. Hence the ANN determines the setpoint for the average temperature based on steady state conditions, some deviation of the maximum temperatures due to dynamic effects remain. Repeating the same current profile daily over a time span of two weeks shows a consistent behavior of the controller. In Figure 9 the daily temperature profiles for $T6$ are plotted. As shown in the Figure the profiles are very similar for each day.

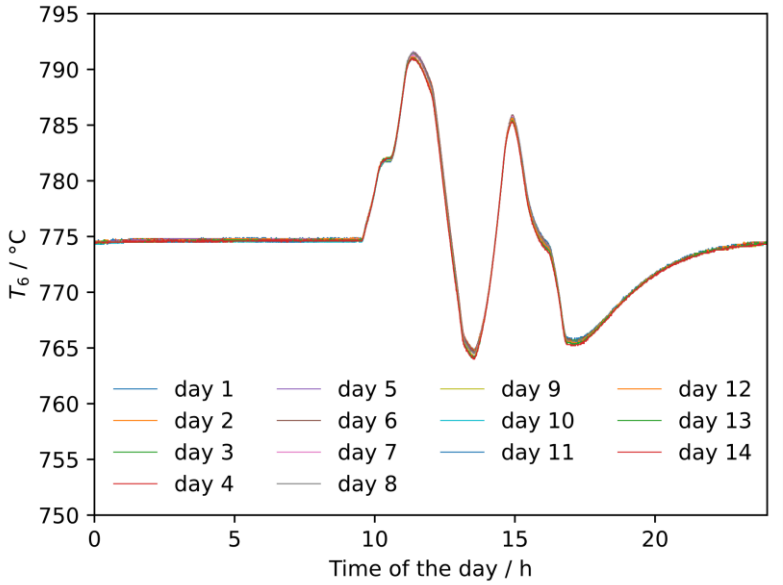

Figure 9. Repeatability of stack temperature *T6* for the daily repeating current profile

Conclusions and Outlook

In this work the authors designed and experimentally evaluated two different controller topologies for fuel cell operation of a reversible solid oxide cell (rSOC) system. The first controller design uses a PID controller to control a weighted average temperature of the IM (stack and heat exchangers). The controller showed in the experiments a very stable and robust behavior. A limitation of this controller is the significant dependency of the maximum temperature on operating conditions like current density. The second design incorporates an ANN for predicting the optimal average temperature to achieve a constant maximum stack temperature. This controller showed a stable behavior as well and reduced the dependency of the maximum stack temperature on operating conditions. Since the ANN predictions are based on steady state data, there remains some minor fluctuation of the maximum temperature during load changes.

To better account for dynamic behavior, future work focuses on real time prediction of dynamic system behavior to control the system based not only on optimal efficiency but also limiting temperature gradient during fast load changes to increase stack lifetime. Furthermore, it is intended to evaluate this controller based on realistic load profiles.

Acknowledgments

The authors would like to thank their colleagues at Forschungszentrum Jülich GmbH for their great support and the Helmholtz Society, the German Federal Ministry of Education and Research as well as the Ministry of Culture and Science of the Federal State of North Rhine-Westphalia for financing these activities as part of the Living Lab Energy Campus. In particular, we would like to thank Mr. Rabah Lekehal and Mr. Stefan Küpper for their help in setting up and operating the demonstration system.

References

1. Ro. Peters, M. Frank, W. Tiedemann, I. Hoven, R. Deja, N. Kruse, Q. Fang, L. Blum and R. Peters, *J. Electrochem. Soc.*, **168**, 014508 (2021).
2. Z. Heydarzadeh, D. McVay, R. Flores, C. Thai and J. Brouwer, *ECS Trans.*, **86** (13), 245 (2018).
3. Y.-D. Kim, J.-I. Lee, M. Saqib, K.-Y. Park, J. Hong, K. J. Yoon, I. Lee and J.-Y. Park, *J. Electrochem. Soc.*, **165**, F728 (2018).
4. A. Hagen, J. V. T. Høgh and R. Barfod, *J. Power Sources*, **300**, 223 (2015).
5. A. Nakajo, Z. Wuillemin, J. Van herle and D. Favrat, *J. Power Sources* 2009, **193**, 203.
6. W. Jiang, Y. Luo, W. Zhang, W. Woo and S. T. Tu, *J. Fuel Cell Sci. Technol.*, **12**, 051004 (2015).
7. R. Peters, W. Tiedemann, I. Hoven, R. Deja, N. Kruse, Q. Fang, L. Blum and R. Peters, *ECS Trans.*, **103** (1), 289 (2021).
8. M. Engelbracht, R. Peters, L. Blum and D. Stolten, *J. Electrochem. Soc.*, **162**, F982 (2015).
9. M. Frank, R. Deja, R. Peters, L. Blum and D. Stolten, *Applied Energy*, **217**, 101 (2018).